




Article

Mollusk Thanatocoenoses Unravel the Diversity of Heterogeneous Rhodolith Beds (Italy, Tyrrhenian Sea)

Valentina Alice Bracchi ^{1,2,*} , Agostino Niyonkuru Meroni ¹ , Vivien Epis ¹ and Daniela Basso ^{1,2} 

¹ Department of Earth and Environmental Sciences, University of Milano-Bicocca, 20126 Milan, Italy; agostino.meroni@unimib.it (A.N.M.); daniela.basso@unimib.it (D.B.)

² Consorzio Interuniversitario per le Scienze del Mare—ConISMa, 00196 Rome, Italy

* Correspondence: valentina.bracchi@unimib.it

Abstract: Emerging evidence of rhodolith bed complexity and heterogeneity poses a challenge to monitoring strategies and questions about the role of abiotic factors in controlling the observed morphostructural diversity. Mollusk thanatocoenoses quickly respond to environmental conditions, expressing fidelity to biocoenosis and representing, thus, a useful ecological/paleoecological tool to unravel this heterogeneity. In this research, we studied three distinct rhodolith beds from the Tyrrhenian Sea (Italy), in a range between 40 and 100 m of water depth, together with their mollusk thanatocoenoses, sediment size, and oceanographic conditions. The beds are all heterogeneous and rarely correspond to a specific rhodolith morphotype and shape. On the contrary, the study of the associated thanatocoenoses led to distinguish at least five different assemblages within the known variability of the Coastal detritic (DC) association. DC and deep mud (VP) mollusk species dominate thanatocoenosis A, which is associated with mixed sediment and a low hydrodynamic regime. Thanatocoenosis B corresponds to an assemblage in which DC species mixed with species of adjacent vegetated bottoms in sandy sediment with a medium hydrodynamic. Thanatocoenosis C includes species related to muddy coastal detritic (DE) and offshore detritic (DL) associated with sand and a variable proportion of praline and branch morphotypes. Thanatocoenoses D and E include a wide range of detritic species (DE DC, DL) together with VP and coralligenous (C), associated with exclusive praline and gravelly sand (Thanat. D), or a mixed proportion of branch and praline and mixed sediment (Thanat. E). Our results demonstrate that the study of mollusk thanatocoenoses provides insights into the diversity within and among heterogeneous rhodolith beds. Moreover, rhodoliths, as part of the sediment, create microhabitats suitable for a wide range of mollusk species that contribute to the formation of complex thanatocoenoses.

Keywords: rhodolith beds; morphotype; mollusk; thanatocoenosis; shape; grain size; currents; Mediterranean benthic bionomics; environmental gradient; habitat heterogeneity



Citation: Bracchi, V.A.; Meroni, A.N.; Epis, V.; Basso, D. Mollusk Thanatocoenoses Unravel the Diversity of Heterogeneous Rhodolith Beds (Italy, Tyrrhenian Sea). *Diversity* **2023**, *15*, 526. <https://doi.org/10.3390/d15040526>

Academic Editor: Fernando Tuya

Received: 10 February 2023

Revised: 21 March 2023

Accepted: 27 March 2023

Published: 5 April 2023



Copyright: © 2023 by the authors. Licensee MDPI, Basel, Switzerland. This article is an open access article distributed under the terms and conditions of the Creative Commons Attribution (CC BY) license (<https://creativecommons.org/licenses/by/4.0/>).

1. Introduction

Rhodoliths are free-living biogenic nodules of calcareous red algae [1]. They are extensively distributed across the Mediterranean Sea, where they form large beds (living rhodoliths >10%) between 9 and 150 m of water depth, typically within 30 and 75 m, and generally located around islands and capes, on top of submarine plateaus, seamounts, marine terraces, channels, and banks [2,3]. In the last three decades, rhodoliths have received more and more attention because their occurrence and three-dimensional structure amplify the complexity of the seafloor as a habitat for a diverse community and a local hotspot of biodiversity, providing a suite of ecosystem goods and services [4]. For these reasons, rhodolith beds have been included in the list of marine benthic habitats of high conservation interest and subjected to a special plan for protection within the framework of the United Nations Program's Mediterranean Action Plan [5,6]. Rhodolith beds are one of the marine habitats included in the monitoring programs of the European Marine Strategy Framework

Directive 2008/56/EC. These beds represent an important transition between soft, mobile substrates and hard, stable ones [7,8]. Interestingly, they display considerable resilience to varying environmental disturbances [9]. Water flows such as waves and currents and bioturbation by benthic vagile invertebrates, and some fish species, have often been indicated as factors that avoid smothering by burial and the overgrowing by other organisms [9–20]. Furthermore, rhodoliths are often associated with sedimentary structures produced by hydrodynamics, such as ripple marks and dunes [13–16]. Up to now, only rare and qualitative indications exist based on field measurements, experimental models, tanks, current velocity, and frequency related to specific rhodolith shapes or morphotypes [21–25]. Consequently, the relationship between rhodolith outer/inner structure and water energy/water depth is still debated, and straightforward paleoenvironmental interpretations based solely on rhodoliths morphology/structure are difficult to achieve [7,26–30]. Each rhodolith presents different features in terms of algal composition (mono- and multi-specific), nucleus (presence/absence/type), morphotype (pralines, branches, and boxwork *sensu* Basso [22,31]), and shape (ellipsoidal, discoidal, spheroidal *sensu* Bosence [32]). These properties should be integrated when discussing the hydraulic behavior of rhodoliths or the relationship between rhodoliths and biota [22,23]. A spherical praline of a given diameter has a much higher density and little internal three-dimensional space available for faunal dwellers compared to a highly branched form (branches = maerl *sensu stricto*) [4,22,23] with the same diameter. Moreover, the comparison of available data of current velocities reveals a difference of one or two orders of magnitude in Atlantic superficial maerl currents vs. Mediterranean deep rhodolith beds currents, which may contribute to explain the variable patterns shown by rhodoliths shape/size along depth gradients [24,25,33].

Several models linking rhodolith shape/size/structure to depth/environmental gradients have been proposed [1,10,14,15,18,23,28,31,32,34–40]. At the bed scale, rhodolith features should be representative, ideally, of a specific combination of environmental conditions. The picture that emerges is instead complex and sometimes contradictory [30], which supports the idea that rhodoliths beds are a largely heterogeneous habitat and that rhodolith morphotypes and shapes observed in each bed do correspond to an unequivocal environmental setting [24]. This is the reason why selecting a model in paleoecological research should be based on careful consideration of the overall environmental context. To overcome this paleoenvironmental limitation, the study of associated biocoenoses and thanatocoenoses (=dead assemblages) could serve as a useful independent tool. Mollusks are generally long-lived organisms that form a well-structured autochthonous assemblage in years or even decades. Such assemblages correspond to local populations composed of individuals of different ages, from juveniles to adults. A well-structured mollusk assemblage requires a quite stable environment, at least at the scale of the mollusks life span [25], but also that the assemblage acquires its character within a biotope that is in dynamic equilibrium, demonstrating both short- and medium-term variability [41]. Considering the time scale for the development of rhodoliths and rhodolith beds (at least few mm y^{-1}), the associated mollusk thanatocoenoses are time-averaged and should reflect their environment over a longer time scale that filters out shorter-term variation and local oscillations [42–46]. Additionally, mollusks often show strong fidelity to specific environmental factors, such as current, input of organic matter, or substrate type and composition that easily outline specific ecological and environmental requirements and paleoecological significance. Lastly, mollusk shells are generally well preserved, and they are objects of several models of benthic zonation, based either on communities [47] or on biocoenosis [48,49], specifically developed for the modern Mediterranean Sea [50,51]. In the framework of the Italian Marine Strategy Framework Program, samples were collected from three rhodolith beds across the Tyrrhenian Sea (Italy), which were partially described in previous papers [24,30]. The current research aims at characterizing the mollusk thanatocoenoses associated with these heterogeneous and complex rhodolith beds with the goal of using them as a tool to decipher analogies and differences within and among beds. This approach can also

represent a key instrument for the paleoenvironmental reconstruction of the abundant rhodolith fossil records.

2. Materials and Methods

2.1. Sampling

Different rhodolith beds were explored in the framework of the Italian Program for the Marine Strategy Framework Directive [52] during several oceanographic cruises between 2017 and 2019 (Figure 1). In all cases, the occurrence of rhodolith beds was confirmed by remote and direct surveys, using a Multibeam Echosounder for the mapping of the extension and Remote Operated Vehicle inspections for ground-truthing [3,24,30]. Rhodoliths from the Pontine Islands were extensively studied [18,31,53], whereas for the Egadi Islands and Sardinia less is known and only partially described in [24,30]. In this research, study locations were denoted as stations (Pontine Island, Egadi Islands, and Sardinia, Figure 1). Within each station, two (Egadi Islands) or three (Pontine Islands and Sardinia) sites were identified. At each site, three replicate samples were collected by a Van Veen grab (30–60 L or by scuba diving, totaling 24 samples. A sub-sample of ca. 200 g was immediately separated from each replicate for grain size analyses and mollusk thanatocoenosis study.

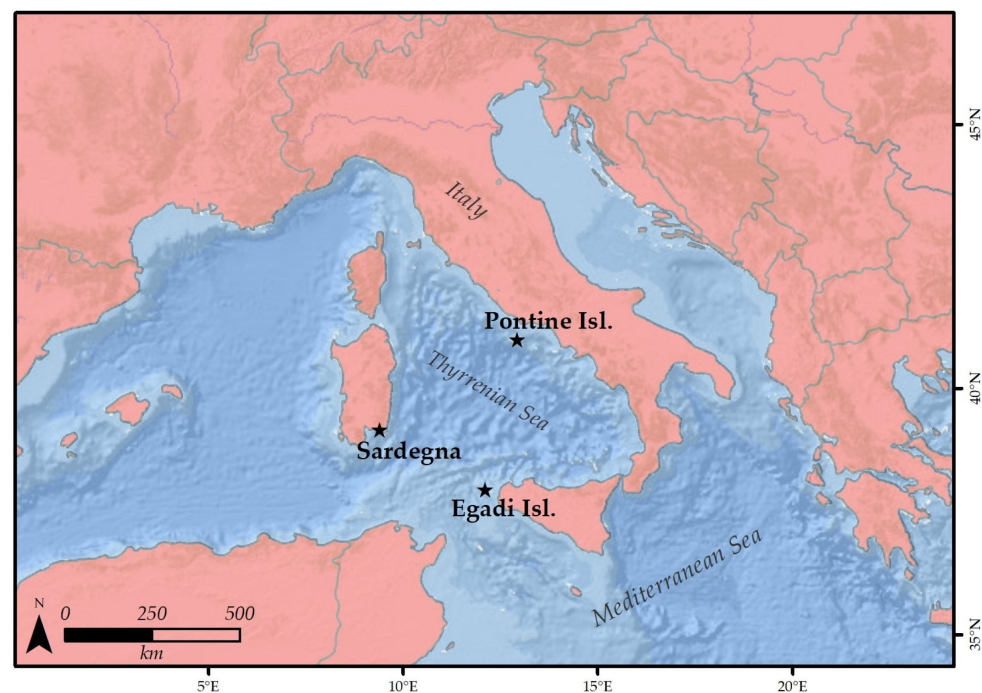


Figure 1. Map with the stations where samples have been collected. Service Layer Credits: Esri, Garmin, GEBCO, NOAA NGDC, and other contributors.

2.2. Rhodoliths

Living rhodoliths were manually collected from each replicate. Each rhodolith was then defined as belonging to boxwork, praline, or branch morphotypes following [3,23,31]. To evaluate rhodolith size and their contributions to the beds, boxwork, and pralines with at least one axis greater than 2 cm were separated and measured along the long (a), intermediate (b), and short (c) axes. These measures were elaborated with TriPlot [54] to define their shape. To reconstruct the coverage of each morphotype within each replicate, all the living rhodoliths, previously separated, were displayed on a sheet of graph paper, one next to the other. We then measured the area covered by each morphotype (cm²). Results were also expressed as percentages. Branches in fruticose rhodoliths were frequently fragmented; therefore, this procedure was not applied to the fruticose morphotype. Branches

were separated into thicker or thinner branches, with a diameter greater or lesser than 0.5 mm, respectively.

2.3. Grain Size and Mollusks

The sub-samples of ca. 200 g, originally separated from each replicate, were used for wet grain size analysis. Mollusk shells were manually sorted from the >1 mm fraction obtained by grain size separation, following Basso and Corselli [44,49] to reconstruct the thanatocoenoses. Mollusk shells were identified with a binocular microscope and counted following [44,49]. Status (J for juvenile, A for adult, and P for population) and conservation (range from 0 to 5) of shells were indicated following [44,49]. Bivalve length and gastropod height were measured to indicate the size of the mollusk shells. Data on their biology, environmental significance, and biocoenosis fidelity *sensu* Pérès and Picard [50] were extracted from the literature [49–51].

2.4. Environmental Data

Oceanographic data (temperature and current referred to the depth at which replicates were collected) were retrieved from a high-resolution physical reanalysis dataset: the MEDSEA product from the Mediterranean Sea Monitoring and Forecasting Centre [55]. The product is based on the Nucleus for European Modeling of the Ocean (NEMO) numerical model with a horizontal grid spacing of $1/24^\circ$ (roughly 5 km) and 141 stretched vertical levels (a higher number of levels is present in the upper 80 m). The numerical model assimilates observations of temperature, salinity, and sea level anomaly. Monthly mean values were extracted in the year of the sampling and in the previous year, according to the sites (2015–2016 for the Egadi and Pontine Islands and 2019–2020 for the Sardinian sites). An area of roughly $25 \text{ km} \times 25 \text{ km}$ centered on each sampling site and at a depth of the samples was defined to average the quantities of interest. This procedure was followed with the aim of reducing the noise derived from relying on a single point of the numerical model. Current velocity was expressed in cm s^{-1} .

2.5. Statistics

Univariate measures of diversity were calculated (total number of species, total number of specimens, Shannon diversity). Multivariate statistics were computed to interpret similarity among stations based on mollusk shells abundance data. The package used for computer statistics was PRIMER v.7 (Plymouth Marine Laboratory). For the multivariate analysis, the pre-treatment of the dataset for mollusks was needed. Species that occurred only as one specimen in one replicate were excluded because they did not contribute to the similarity [44,49,56,57]. Species occurring only as juvenile specimens were also excluded because of their poor contribution to the environmental interpretation. Moreover, we also excluded those species that were ubiquitous and often present with high numbers of specimens (e.g., *Bittium reticulatum*) because their numerical dominance masked the structure of the shell assemblage [56,57]. This reduced dataset was named Reduction 1. We also extracted from the whole dataset only those species that expressed specific fidelity to biocoenosis in the framework of the benthic marine bionomics [49–51]. This reduced dataset was named Reduction 2. In the framework of a quantitative approach, a first hierarchical agglomerative clustering and non-metric multidimensional scaling (MDS) ordination were performed on both datasets of double square root transformed abundance data. Cluster analysis based on Bray–Curtis similarity has been used for the hierarchical classification of mollusk abundance data. The MDS is a non-parametric method that uses the rank order of similarities between samples rather than their absolute values. The method was considered to be statistically very robust and sensitive in community studies [56,57]. Double square root transformation reduces the over-representation of ubiquitous and abundant species, and when coupled with the Bray–Curtis similarity index, the obtained similarity coefficient is invariant to a scale change (e.g., the dimension of the sample) [56]. The most important

species were identified on the base of their contribution to the similarity/dissimilarity within and between the clusters.

An environmental dataset for the same stations was created, including morphotype coverage (percentage per morphotype per replicate), grain size (mud, sand, and gravel percentage), depth, current (cm s^{-1}), and temperature ($^{\circ}\text{C}$) (minimum, maximum, and mean values considering 2 years). Principal component analysis (PCA) was conducted to explore which factor drove the differences among replicates, sites, and stations.

3. Results

3.1. Rhodoliths

Rhodolith morphotype coverage at the studied stations indicated that the beds were generally heterogeneous (Figure 2). Praline was the most abundant morphotype but exclusive only at site Egadi2, followed by branch (Figure 2). Moreover, pralines were often smaller than 2 cm (Supplementary File S1). Branches were common but abundant only at site Pontine2, where they were generally thicker than in the other sites (Supplementary File S1). Boxwork morphotype was rarer and basically only appeared in the sites Egadi1 and Santa Caterina (Figure 2). Boxworks often had dimensions greater than 2 cm (Supplementary File S1). Moreover, considering praline and boxwork with at least one axis greater than 2 cm, TRIplot diagrams (Figure 3) showed a strong heterogeneity in terms of shape (Figure 3). Only Sardinian rhodoliths significantly approached the sub-spheroidal to spheroidal shape (Figure 3).

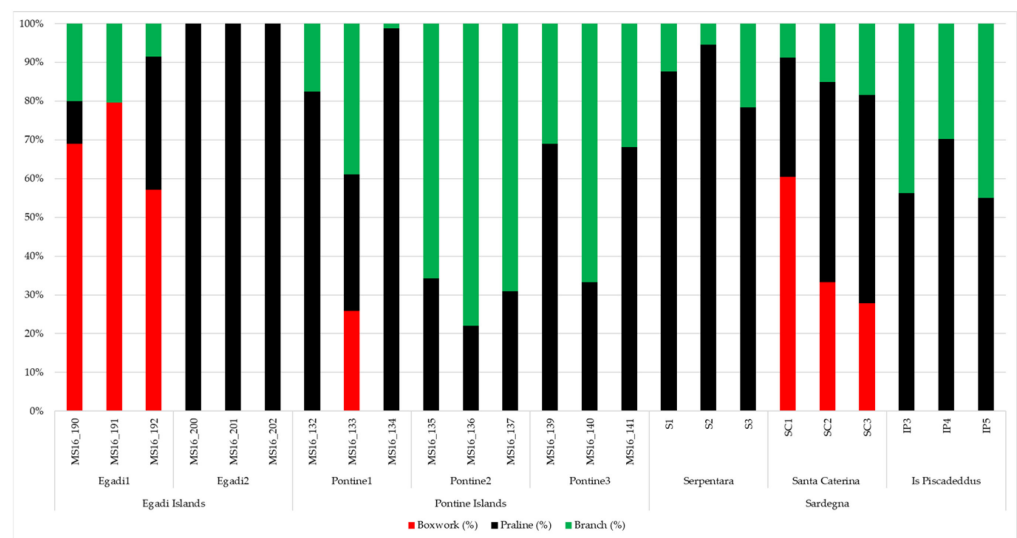


Figure 2. Bar graph with the morphotype coverage per station and site. Red is for boxwork, black is for pralines, and green is for branches.

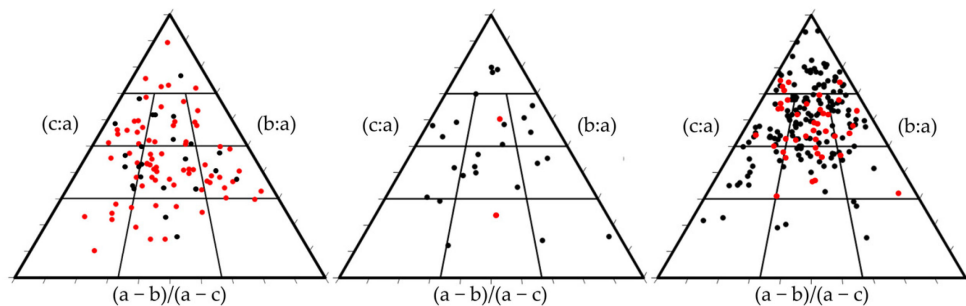


Figure 3. Triplot graphs with rhodolith (only >2 cm) shapes at Egadi, Pontine, and Sardinia stations, respectively. Black is for pralines, and red is for boxworks.

3.2. Mollusks

The identified mollusk thanatocoenoses totaled 197 species and 5731 specimens (Table 1, Supplementary File S2). The number of species per replicate ranged between 12 (MS16_132) and 52 (SC3); the number of specimens per replicate ranged between 46 (MS16_132) and 774 (Supplementary File S2) (Table 1, Supplementary File S2). More bivalves than gastropods characterized the Egadi station, whereas the opposite was for both the Pontine and Sardinia stations (Supplementary File S2). Mollusk shells were often adult shells or representative of a wide size corresponding to population (Supplementary File S2). Bivalve length ranged between 1 mm and 1 cm, with a mean value <5 mm; gastropods height ranged between 1 mm and 2 cm, with a mean value of 4 mm. Sardinia station had the highest species richness (136) with respect to Egadi (93) and Pontine (72) stations. Shannon diversity ranged between 0.58 (MS16_141) and 0.95 (SC1) (Table 1). The cluster analysis based on the dataset Reduction 1 identified six clusters of replicates at 25% of Bray–Curtis similarity (Figure 4, Supplementary File S2). A dendrogram based on dataset Reduction 2 (Figure 5, Supplementary File S3) identified five clusters with a higher similarity rank (40%). The two SIMPER analyses identified the species that mostly drove the clustering (Supplementary Files S4 and S5).

Table 1. List of stations, sites, and replicates with the indication of depth, location, number of identified species, specimens abundance, and Shannon Diversity Index.

Station	Site	Replicate	Depth (m)	Latitude	Longitude	Species	Abundance	Shannon Index
Egadi Islands	Egadi1	MS16_190	103	37.9236	12.1412	38	243	0.79
		MS16_191	102.8	37.9236	12.1412	35	161	0.81
		MS16_192	103.1	37.9236	12.1412	35	142	0.77
	Egadi2	MS16_200	86.5	37.9500	12.1205	35	162	0.85
		MS16_201	86.5	37.9500	12.1205	39	296	0.80
		MS16_202	86.5	37.9501	12.1205	31	208	0.84
Pontine Islands	Pontine1	MS16_132	66.6	40.9102	12.8693	12	46	0.81
		MS16_133	66.9	40.9102	12.8693	26	153	0.74
		MS16_134	66.9	40.9102	12.8693	28	124	0.74
	Pontine2	MS16_135	65.9	40.9155	12.8853	15	65	0.84
		MS16_136	66.4	40.9155	12.8854	17	214	0.71
		MS16_137	66.1	40.9155	12.8853	14	96	0.86
	Pontine3	MS16_139	65	40.9113	12.8828	27	177	0.69
		MS16_140	64.9	40.9113	12.8829	24	175	0.66
		MS16_141	64.8	40.9113	12.8828	31	384	0.66
Sardinia	Serpentara	S1	59	39.1499	9.6127	44	618	0.58
		S2	59	39.1499	9.6127	45	774	0.60
		S3	59	39.1499	9.6127	43	712	0.58
	Santa Caterina	SC1	40	39.0865	9.4966	32	57	0.95
		SC2	40	39.0863	9.4964	20	35	0.86
		SC3	40	39.0861	9.4963	52	682	0.64
	Is Piscadeddus	ISPIS3	45	36.1120	9.4518	16	70	0.77
		ISPIS4	45	36.1120	9.4518	22	80	0.76
		ISPIS5	45	36.1074	9.4558	18	57	0.79

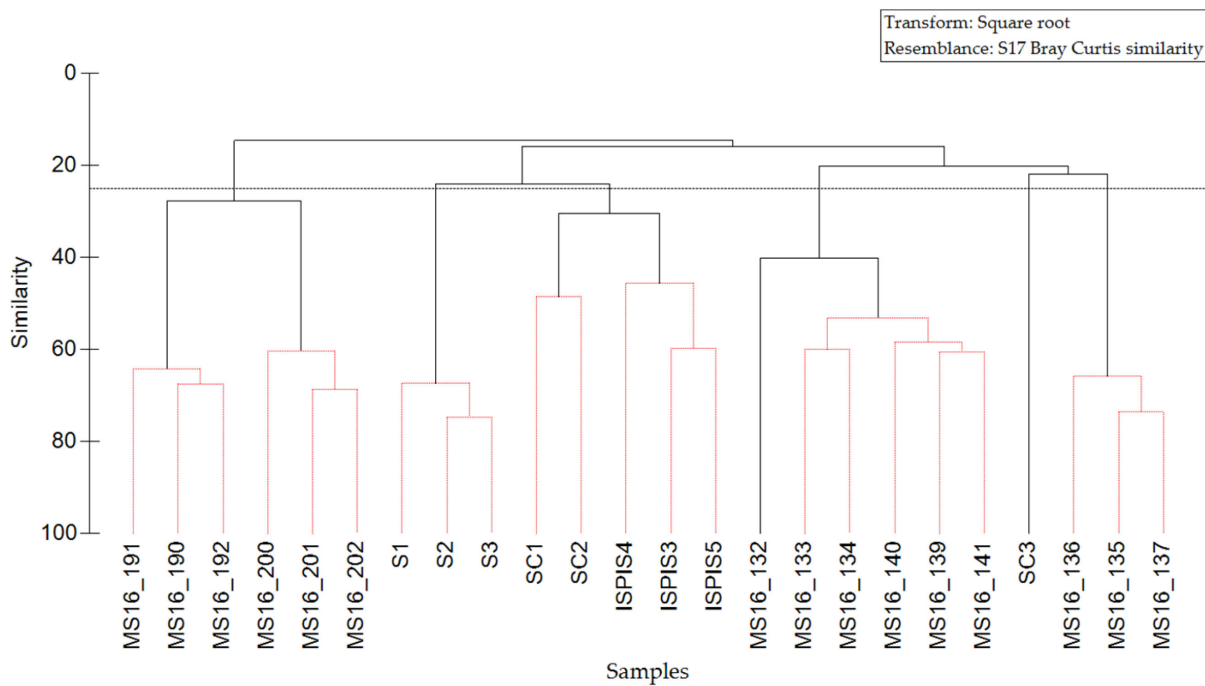


Figure 4. Dendrogram based on the dataset Reduction 1. Similarity cut at 25%.

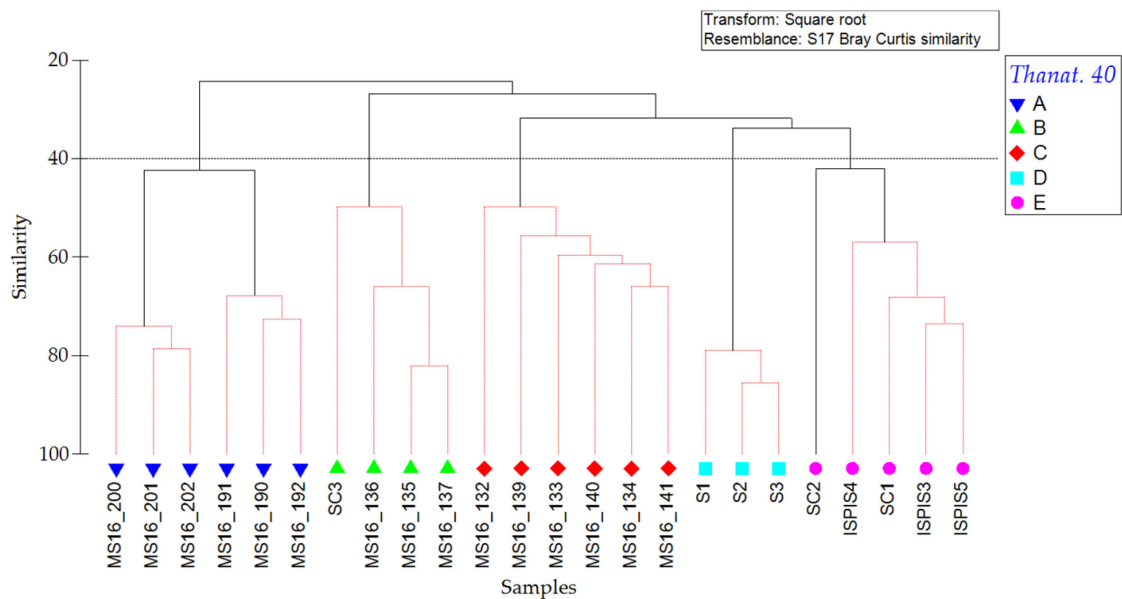


Figure 5. Dendrogram based on dataset Reduction 2. Similarity cut at 40%; it identifies five thanatocoenoses (A–E).

Thanatocoenosis A (Figure 5) included all the replicates from Egadi station, where the following mollusk species were exclusive or strictly abundant: *Astarte sulcata* (exclusive coastal detritic—DC), *Melanella polita* (exclusive DC), *Asperarca secreta* (preferential DC), *Archimediella triplicata* (exclusive DC), *Tetrarca tetragona* (preferential DC), and *Limatula subauriculata* (exclusive deep mud—VP) (Supplementary File S4). Among the other species, the most significant in distinguishing this cluster were *Heteranomina squamula* and *Neolepton sulcatum* (Supplementary File S5).

Thanatocoenosis B (Figure 5) included all the replicates of site Pontine2 together with all replicates of site SC3. There were some exclusive species, such as *Alvania cimex* (*Posidonia* meadows—HP) and *Striarca lactea* (photophilous algae—AP, HP), together with

some others with a high abundance, such as *Jujubinus exasperatus* (HP) and *Bolma rugosa* (exclusive DC) (Supplementary File S4). Among the other species, the most significant in distinguishing this cluster were *Alvania beanii*, *Mysia undata*, and *Parvicardium scabrum* (Supplementary File S5).

Thanatocoenoses C–E (Figure 5) shared the occurrence of *Timoclea ovata* (DE, DL) and *Mimachlamys varia* (preferential offshore detritic—DL), together with a high abundance of *Papillicardium papillosum* (preferential DC). Thanatocoenoses D and E shared *Alvania cimicooides* (preferential DC, DL, VP), *Moerella donacina* (exclusive DC) and *Palliolum incomparabile* (exclusive coralligenous—C) (Supplementary File S4). Moreover, *G. triangularis* (exclusive coarse sand and fine gravel under the influence of bottom current, SGCF), *Clausinella fasciata* (preferential SGCF), *A. beanii* and *Diplodonta rotundata* characterized thanatocoenosis C, and *Digitaria digitaria* thanatocoenoses D and E (Supplementary File S5).

3.3. Grain Size

Sediment associated with rhodolith beds was sand at Pontine station (thanatocoenoses B and C), whereas gravelly sand occurred at site Egadi2, Serpentara (thanatocoenosis D), and Santa Caterina (thanatocoenoses B and E). Mixed sediment (muddy-gravelly sand) occurred at site Egadi1 and Is Piscadeddus (thanatocoenoses A and E) (Figure 6, Supplementary File S3).

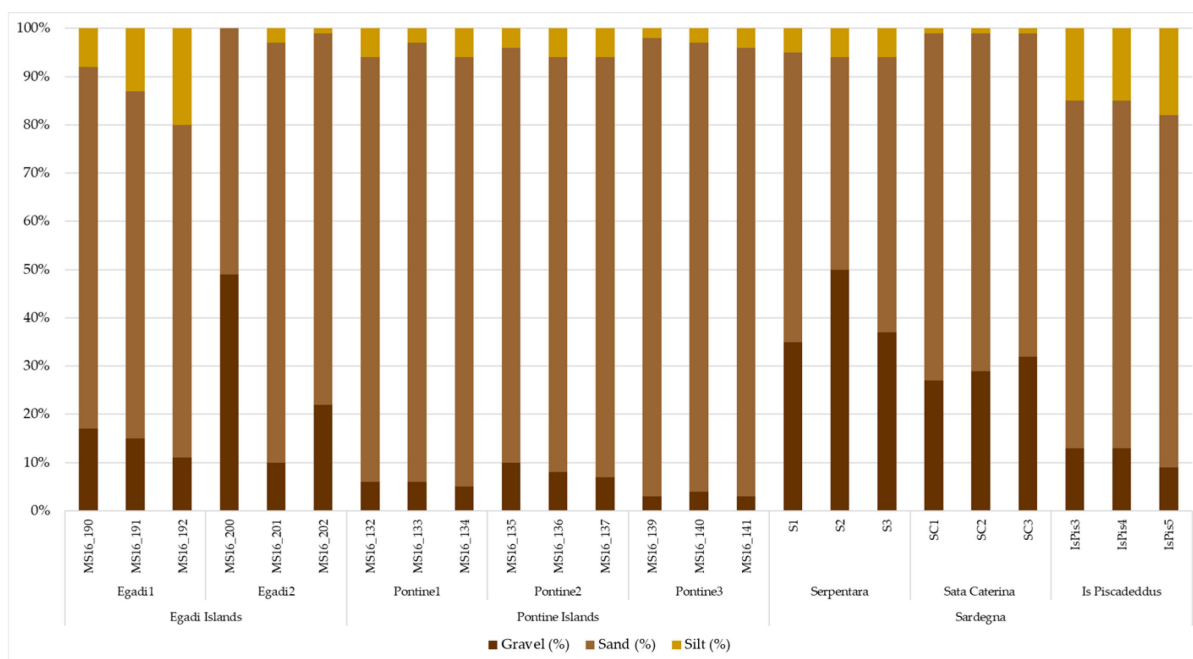


Figure 6. Bar graph with the grain size percentage per station and site.

3.4. Environmental Data

Samples were collected at water depths ranging between 40 and 103 m (Table 1) across the whole Tyrrhenian Sea. Temperature patterns were very similar between the Pontine Islands and Sardinia stations (Supplementary File S3), whereas maximum values were much higher at Egadi Islands (up to 21.1 °C, Supplementary File S3). Currents had different velocities among the studied stations (Figure 7). Minimum currents ranged between 0.4 cm s⁻¹ (Pontine2) and 2.4 cm s⁻¹ (Pontine1, Egadi1, and Egadi2) (Figure 8). The maximum value was reached at the Serpentara site (17.7 cm s⁻¹) (Figure 7). Current was generally higher at Egadi Islands (mean = 11.2 cm s⁻¹), whereas, at the Pontine station, it ranged between 5.7 and 11.2 cm s⁻¹ (Supplementary File S3).

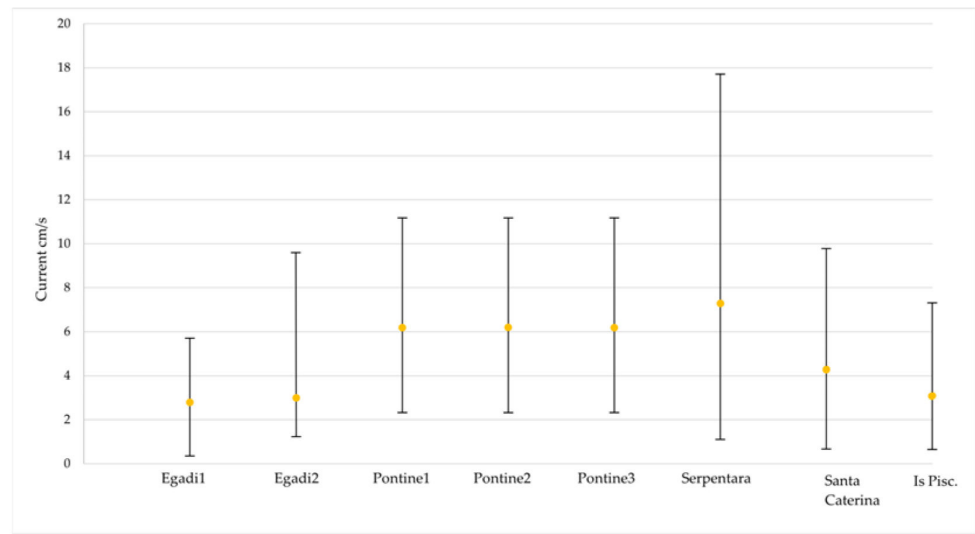


Figure 7. Scatter plot of mean current velocity per site. Bars indicate the range with the minimum and the maximum values. Measure unit: cm s^{-1} .

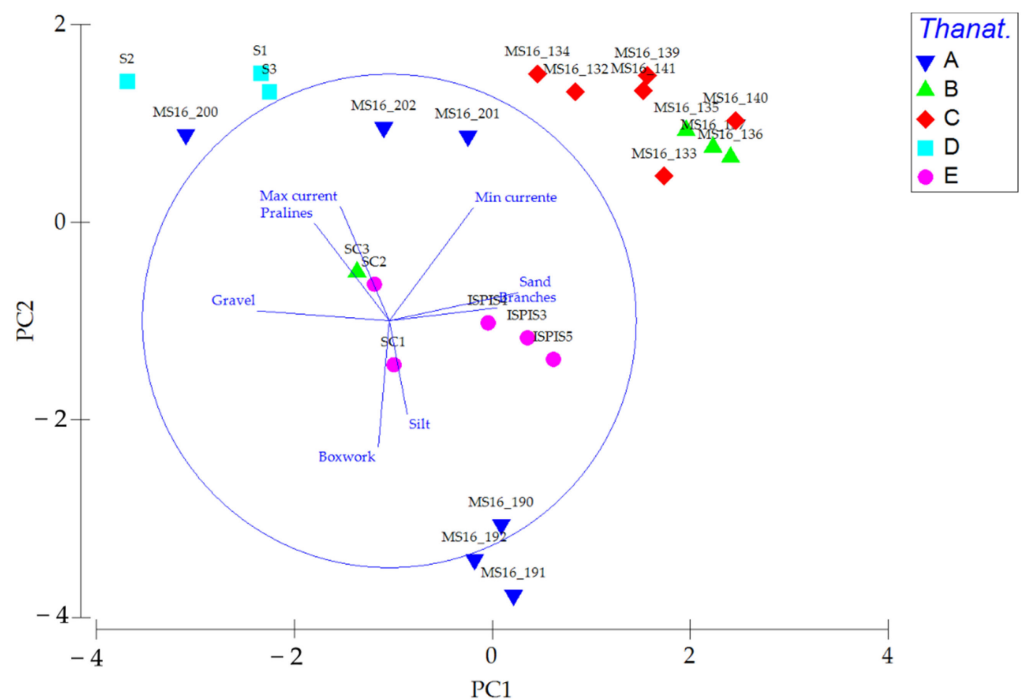


Figure 8. Graph of the principal component analysis that considers all the environmental data (current values, grain size, depth), together with morphotype coverage values.

PCA identified the most important drivers of diversity among replicates. PCA1 corresponded to gravel and sand percentages and the occurrence of branch morphotypes (Figure 8). PCA2 corresponded to mud percentage, the occurrence of boxwork, and minimum/maximum current values (Figure 8). Thanatocoenosis B and C were all in the top-right (Figure 8) because of sand (Thanatocoenosis C, red rhombus) and branch morphotype (Thanatocoenosis B, green triangles) contribution. Only replicate SC3 was placed distant from the other replicates of the same thanatocoenosis and station because of different percentages of gravel. Thanatocoenosis D was in the top-left because of the higher hydrodynamics, together with the high praline percentage. Thanatocoenosis E gathered in the middle, whereas thanatocoenosis split into two subgroups representative of the two sites, Egadi1 below and Egadi2 top, respectively, along the PC2 axis. Egadi1

(thanatocoenosis A below) had more boxwork like SC1 and SC2, a low hydrodynamic and muddy-gravelly sand like the ISPIS site (Figure 8). Egadi2 (thanatocoenosis A top) had no boxwork like the ISPIS site and was gravelly sand and hydrodynamic like SC1 and SC2 (Figure 8).

4. Discussion

Heterogeneity characterizes the studied rhodolith beds in terms of rhodolith morphotypes and shape (Figures 2 and 3, Supplementary Files S1 and S2). This suggests that despite a similar depth (Table 1) or similar current values (Figure 8), non-univocal combinations of rhodolith coverage can be expected. Hydrodynamics is generally indicated as one of the most important drivers for rhodoliths growth and survival. Since rhodoliths are able to cover a wide bathymetric range [1], the current speed values can differ a lot, for example, between the Atlantic Ocean ([24], order of m s^{-1}) and the Mediterranean Sea (this paper, order of cm s^{-1}), leading to different conclusions on the relation between hydrodynamics and habitat complexity. Consequently, the exclusive use of morphometric rhodolith features is not exhaustive to reconstruct environmental/paleoenvironmental conditions. This has to be considered in the framework of the study of a rhodolith bed, its description, and characterization, as well as in the management and conservation of these important habitats [3,24].

In this paper, we consider rhodoliths as elements composing the sedimentary substrate, having an obvious influence on the associated mollusk biocoenoses/thanatocoenoses. Considering the size of most of the mollusk shells, each rhodolith acts as a complex of microhabitats. In the three-dimensional structure of the rhodolith, a mollusk can find a niche for its survival that does not correspond to the surrounding seafloor substrate [58]. For example, in the voids and microcavities of boxwork rhodoliths, local mud accumulation supports VP species (Thanatocoenosis A). Moreover, the complex surface of pralines mimicking a small build-up can support C species (Thanatocoenosis E). This suggests that the occurrence of rhodoliths and their structural heterogeneity contribute to creating a very complex suite of substrates, even at the same site, where species linked to different biocoenoses can occur closely, contributing to the formation of complex thanatocoenoses. Another interesting consideration is that the complete list of mollusk thanatocoenoses is dominated by species related to “hard substrate” (Supplementary File S2). At the scale of the mollusk size, the coarse fraction (gravel) of the sediments, largely composed of rhodoliths, represents the suitable (in term of size) hard substrate to support such species. This also suggests that rhodoliths highly influence mollusk distribution.

The study of mollusk thanatocoenoses associated to rhodolith beds can be a powerful tool to complement this approach because of their fidelity to edaphic factors and oceanographic conditions and their ability to respond quickly to environmental change (Table 2). In our study, the Shannon Index of mollusk thanatocoenoses shows variable values (Table 1). The lowest values have been found at the Serpentara site (0.58), which interestingly corresponds to the site where currents reach maximum values (Figure 7), and rhodolith morphotypes are quite exclusive (Figure 2, Supplementary File S1). Higher hydrodynamics can affect the stability of the rhodoliths, bringing to fragmentation of the habitat itself and consequently to a paucity of mollusk thanatocoenoses. The higher values of this index are less straightforward. We can infer that a higher substrate complexity, such as the one provided by the heterogeneous shape and morphotype of the studied rhodoliths (where boxwork are abundant, for example, at site Egadi1), or associated with mixed sediment, can support a higher mollusk biodiversity. Moreover, in this research, we considered thanatocoenoses to be representative also of spatially averaged properties because of the mosaicking seascape made of different adjacent habitats, which can partially contribute to the biodiversity increase. This can be the case for thanatocoenosis B, which includes several mollusk species belonging to AP/HP biocoenoses (Table 2).

Table 2. A summary of the main features related to the identified thanatocoenoses. “Thanat.” in the first column is s for thanatocoenosis.

Thanat.	Species	Sediment	Morphotype	Current
A	DC/VP	Mixed	Boxwork-praline	Medium-low
B	AP/HP/DC	Sand	Branch-praline	Medium-high
C	DE/DL/SGCF	Sand	Praline-branch	Medium-high
D	DE/DL/DC/VP	Gravelly sand	Praline	High
E	DE/DL/DC/VP/C	Mixed	Praline-branch	Medium

The statistical treatment of the mollusk abundance identifies several distinctive thanatocoenoses corresponding to different combinations of environmental drivers (Table 2) within the known variability of the DC association [41]. Interestingly, the cluster analysis performed on Reduction 2, a subset list of ecologically significant mollusk species (Figure 5), identifies 5 thanatocoenoses at 40% of similarity and appears more informative than the cluster analysis performed on the whole dataset (Figure 4). This confirms the usefulness of marine bionomics as a tool to interpret the main significance of thanatocoenoses, associated sediment, and environmental/paleoenvironmental conditions [45,46,59]. Thanatocoenosis A corresponds to a DC/VP assemblage that characterizes the whole Egadi station, where rhodoliths have different features. In fact, typical DC facies with exclusive pralines occurs at the site Egadi1 [50,51]. In this specific case, the rhodolith morphotype and mollusk thanatocoenosis match very well. Moreover, at Egadi1, the associated sediment is sandier than in Egadi2, where boxworks and a higher percentage of mud are indicated, supporting the occurrence of also VP species as well. Thanatocoenosis B also includes DC species but with an abundant stock of species related to AP and HP biocoenoses. As already indicated before, this can be the result of mixing due to a coeval source of mollusk shells from adjacent vegetated habitats. A more complex assemblage characterizes thanatocoenoses C-E, which points to the mixing of circalittoral species. In particular, all three thanatocoenoses list species related to muddy detritic bottoms (DE, DL) (Figure 5, Supplementary Files S2–S5), together with DC species (thanatocoenoses D and E) and C species (Thanatocoenosis E). The mixing of species related to different biocoenoses suggests that environmental conditions at the corresponding sampling sites can significantly vary.

The statistical analysis supports the identification of patterns between thanatocoenoses and environmental drivers (Figures 7 and 8, Supplementary File S6). Depth, although statistically significant, cannot be considered a discriminant because, from the ecological point of view, it is a gradient along which the relevant drivers vary (Figures 7 and 8). Grain size associated with thanatocoenoses results to be statistically significant in distinguishing the assemblages, together with the values of maximum and minimum current speed (Figures 7 and 8, Supplementary File S6). The occurrence of gravel is associated with DC mollusk species being locally dominant (thanatocoenosis A). In the case of mixed sediment, VP species (thanatocoenosis A) or a wider assemblage of species (thanatocoenoses D and E) occurs. DC/VP species (thanatocoenosis A) characterizes the boxwork-dominated rhodolith bed in the site Egadi1, whereas thanatocoenosis B (DC + AP/HP) identifies a branch-dominated bed. These observations confirm the validity of the model of distribution of rhodolith morphotypes [30] based on two main drivers (hydrodynamics and sediment grain size) in the framework of Mediterranean bionomics. Incidentally, where praline is the most abundant morphotype, the correspondent thanatocoenoses show the different contributions of DC, DE, DL, and C species. The relation between identified thanatocoenoses and hydrodynamics is not univocal (Table 2). Thanatocoenosis A is characterized by the lowest hydrodynamic regime (Figure 7). This condition supports both the occurrence of boxwork morphotype and mud-loving species (VP). Thanatocoenoses B and C have medium-high current values, and they are mostly related to pure sand and higher branch coverage. Thanatocoenosis D includes species associated with the highest

hydrodynamic (Table 2), with rhodoliths characterized by quite exclusive small praline (Figure 2) and gravelly sand sediments supporting a thanatocoenosis in which DE and DL species are dominant. Interestingly, thanatocoenosis D, which occurs at the site with the highest current values (Figure 7), does not contain any mollusk species of biocoenoses strictly related to currents such as SGCF (Table 2). On the contrary, they occurred only in thanatocoenosis C, where they are never statistically significant or with only juvenile specimens/one occurrence (Table 2). This suggests that, although the highest values of currents are observed where thanatocoenosis D occurs (Figure 7), these highest peaks are only sporadic and do not support the occurrence of specific-related mollusk species.

5. Conclusions

Heterogeneous rhodolith beds, not easily distinguishable based on the dominant rhodolith shape/morphotype within and among beds, are associated with at least five different mollusk thanatocoenoses. Subtle but effective differences exist among environmental conditions at the studied stations, together with a different sedimentary regime. All five different thanatocoenoses point to a circalittoral environment within the known variability of the DC association. DC/VP species strongly distinguish thanatocoenosis A, while a suite of features and drivers control the separation of the other assemblages, such as the proximity of photophilous environments (thanatocoenosis B), a more mixed sediment and medium hydrodynamic (thanatocoenosis E), a higher percentage of gravel and a more intense hydrodynamic regime (thanatocoenosis D), and sandier sediment (thanatocoenosis C). Being the rhodoliths part of the sediment itself, they provide microhabitats that are suitable for a wide and variegated range of mollusk species than expected, and consequently, the occurrence of complex thanatocoenoses. Moreover, our results support that the study of mollusk thanatocoenoses provides evident insights within and among heterogeneous rhodolith beds, that can be of support also for paleoenvironmental reconstruction.

Supplementary Materials: The following supporting information can be downloaded at: <https://www.mdpi.com/article/10.3390/d15040526/s1>. Supplementary File S1: Data on rhodolith morphotype, shape, and coverage. Supplementary File S2: Complete list of the mollusk species, the Abundance (A, sx is for left valve, dx is for right valve), together with the indication of Status (S), Conservation (C), Biocoenosis, Habitus, and Edaphic preferences per site. In biocoenosis: AP is for photophilous algae, HP is for *Posidonia* meadows, SFBC is for fine well-sorted sand, SVMC is for shallow muddy sand under low hydrodynamic, C is for coralligenous, DC is for coastal detritic, DL is for offshore detritic, DE is for muddy detritic, VTC is for coastal terrigenous mud, VP is for deep mud, and SGCF is for coarse sand and fine gravel under bottom currents. “Sspr” is for species that do not have a precise ecological meaning, “lre” is for species that have a large ecological distribution, “excl” is for exclusive species, “pref” is for preferential species, and “acc” is for accidental species. Supplementary File S3: List of the subset of mollusk with expressed fidelity in the benthic marine bionomy system of Pérès and Picard (1964) (Abundance), together with the data on environmental parameters (depth in m, current in cm s^{-1} , and temperature in $^{\circ}\text{C}$) and grain size results (percentage). Supplementary File S4: Results of the SIMPER test for mollusk dataset “Reduction 1” and Cluster analysis cut at 25% of similarity. Supplementary File S5: Results of the SIMPER test for mollusk dataset “Reduction 2” and Cluster analysis cut at 40% of similarity. Supplementary File S6: MDS graphs with the overlaid contribution (pink bubbles) of Boxworks, Pralines, and Branches (%), grain size (%), and currents (cm s^{-1}). For absolute values, please refer to Supplementary File S3. Overlay clustering (green line) is with a similarity of 40% for mollusk dataset “Reduction 2”.

Author Contributions: Conceptualization V.A.B. and D.B.; methodology, V.A.B., A.N.M., V.E. and D.B.; software, V.A.B., A.N.M. and D.B.; formal analysis, V.A.B. and D.B.; investigation, V.A.B.; data curation, V.A.B. and D.B.; writing—original draft preparation, V.A.B. and D.B.; writing—review and editing, V.A.B., A.N.M. and D.B.; visualization, V.A.B. and D.B.; funding acquisition, D.B. All authors have read and agreed to the published version of the manuscript.

Funding: This research was funded in the framework of the agreement between the University of Milano-Bicocca and the “Capo Carbonara” Marine Protected area “Convenzione Operativa tra L’area Marina Protetta “Capo Carbonara” e L’università degli Studi di Milano-Bicocca per la Realizzazione

delle Attività di Monitoraggio e Ricerca Sulla Strategia Marina”, grant number 2017-CONV25-0092. Samples from Egadi and Pontine Islands have been collected in the framework of the activities for the “Convenzione MATTM-CNR per i Programmi di Monitoraggio per la Direttiva sulla Strategia Marina (MSFD, Art. 11, Dir. 2008/56/CE)”.

Institutional Review Board Statement: Not applicable.

Data Availability Statement: The data presented in this study are available in Supplementary Files S1–S3.

Acknowledgments: We are thankful to Fernando Tuya and two anonymous reviewers for helpful suggestions during the first revision of the manuscript. For the sample from Pontine and Egadi Islands, the captain, crew and scientific staff of RV Minerva Uno cruise STRATEGIA MARINA LIGURE-TIRRENO are acknowledged for their efficient and skillful cooperation at sea. We thank the crew of the “Capo Carbonara” Marine Protected Area for their help during the sampling activity at Sardegna station.

Conflicts of Interest: The authors declare no conflict of interest.

References

- Bosellini, A.; Ginsburg, R.N. Form and Internal Structure of Recent Algal Nodules (Rhodolites) from Bermuda. *J. Geol.* **1971**, *79*, 669–682. [[CrossRef](#)]
- Foster, M.S.; Amado Filho, G.M.; Kamenos, K.A.; Riosmena-Rodríguez, R.; Steller, D.L. Rhodoliths and Rhodolith Beds. In *Research and Discoveries: The Revolution of Science Through SCUBA*; American Academy of Underwater Sciences: Mobile, AL, USA, 2013; pp. 143–155.
- Basso, D.; Babbini, L.; Ramos-Esplá, A.A.; Salomidi, M. Mediterranean Rhodolith Beds. In *Rhodolith/Maërl Beds: A Global Perspective*; Riosmena-Rodríguez, R., Nelson, W., Aguirre, J., Eds.; Coastal Research Library; Springer: Cham, Switzerland, 2017; Volume 15, pp. 281–298.
- Riosmena-Rodríguez, R.; Nelson, W.; Aguirre, J. *Rhodolith/Maërl Beds: A Global Perspective*; Springer International Publishing: Cham, Switzerland, 2017. [[CrossRef](#)]
- Basso, D.; Babbini, L.; Kaleb, S.; Bracchi, V.A.; Falace, A. Monitoring deep Mediterranean rhodolith beds. *Aquat. Conserv. Mar. Freshw. Ecosyst.* **2015**, *26*, 549–561. [[CrossRef](#)]
- UNEP-MAP-RAC/SPA. *Action Plan for the Conservation of the Coralligenous and Other Calcareous Bio-Concretions in the Mediterranean Sea*; Pergent-Martini, C., Brichet, M., Eds.; RAC/SPA: Tunis, Tunisia, 2008; p. 21.
- Basso, D.; Nalin, R.; Massari, F. Genesis and composition of the Pleistocene Coralligène de plateau of the Cutro Terrace (Calabria, southern Italy). *Neues Jahrb. Für Geol. Und Paläontologie–Abh.* **2009**, *244*, 73–182. [[CrossRef](#)]
- Foster, M.S. Rhodoliths: Between Rocks and Soft Places. *J. Phycol.* **2001**, *37*, 659–667. [[CrossRef](#)]
- Steller, D.L.; Riosmena-Rodríguez, R.; Foster, M.S.; Roberts, C.A. Rhodolith bed diversity in the Gulf of California: The importance of rhodolith structure and consequences of disturbance. *Aquat. Conserv. Mar. Freshw. Ecosyst.* **2003**, *13*, S5–S20. [[CrossRef](#)]
- Bosence, D.W.J. Ecological studies on two unattached coralline algae from Western Ireland. *Palaeontology* **1976**, *19*, 365–395.
- BIOMAERL Team. Conservation and management of northeast Atlantic and Mediterranean maërl beds. *Aquat. Conserv. Mar. Freshw. Ecosyst.* **2003**, *13*, S65–S76. [[CrossRef](#)]
- Bordehore, C.; Borg, J.A.; Lanfranco, E.; Ramos-Esplá, A.A.; Rizzo, F.; Schembri, P.J. Trawling as a major threat to Mediterranean maërl beds. In *Proceedings of the First Mediterranean symposium on Marine Vegetation, Mednature, Ajaccio, France, 3–4 October 2000*; Volume 1, pp. 105–109.
- Bordehore, C.; Ramos-Esplá, A.A.; Riosmena-Rodríguez, R. Comparative study of two maërl beds with different otter trawling history, southeast Iberian Peninsula. *Aquat. Conserv. Mar. Freshw. Ecosyst.* **2003**, *13*, S43–S54. [[CrossRef](#)]
- Bahia, R.G.; Abrantes, D.P.; Brasileiro, P.S.; Filho, G.H.P.; Filho, G.M.A. Rhodolith bed structure along a depth gradient on the northern coast of Bahia state, Brazil. *Braz. J. Oceanogr.* **2010**, *58*, 323–337. [[CrossRef](#)]
- Riul, P.; Targino, C.H.; Farias, J.D.N.; Visscher, P.T.; Horta, P.A. Decrease of Lithothamnion sp. (Rhodophyta) primary production due to the deposition of a thin sediment layer. *J. Mar. Biol. Ass. UK* **2008**, *88*, 17–19. [[CrossRef](#)]
- Barberá, C.; Moranta, J.; Ordines, F.; Ramón, M.; de Mesa, A.; Díaz-Valdés, M.; Grau, A.M.; Massutí, E. Biodiversity and habitat mapping of Menorca Channel (western Mediterranean): Implications for conservation. *Biodivers. Conserv.* **2012**, *21*, 701–728. [[CrossRef](#)]
- Micallef, A.; Le Bas, T.P.; Huvenne, V.A.; Blondel, P.; Hühnerbach, V.; Deidun, A. A multi-method approach for benthic habitat mapping of shallow coastal areas with high-resolution multibeam data. *Cont. Shelf Res.* **2012**, *39–40*, 14–26. [[CrossRef](#)]
- Sañé, E.; Chiocci, F.; Basso, D.; Martorelli, E. Environmental factors controlling the distribution of rhodoliths: An integrated study based on seafloor sampling, ROV and side scan sonar data, offshore the W-Pontine Archipelago. *Cont. Shelf Res.* **2016**, *129*, 10–22. [[CrossRef](#)]
- Millar, K.; Gagnon, P. Mechanisms of stability of rhodolith beds: Sedimentological aspects. *Mar. Ecol. Prog. Ser.* **2018**, *594*, 65–83. [[CrossRef](#)]

20. O'Connell, L.G.; James, N.P.; Harvey, A.S.; Luick, J.; Bone, Y.; Shepherd, S.A. Reevaluation of the Inferred Relationship Between Living Rhodolith Morphologies, Their Movement, and Water Energy: Implications for Interpreting Paleooceanographic Conditions. *Palaios* **2020**, *35*, 543–556. [[CrossRef](#)]
21. Marrack, E.C. The Relationship between Water Motion and Living Rhodolith Beds in the Southwestern Gulf of California, Mexico. *Palaios* **1999**, *14*, 159–171. [[CrossRef](#)]
22. Basso, D.; Tomaselli, V. Paleocological potentiality of rhodoliths: A Mediterranean case history. *Boll. Soc. Paleontol. Ital.* **1994**, *2*, 17–27.
23. Basso, D.; Nalin, R.; Nelson, C.S. Shallow-water *Sporolithon* rhodoliths from north island (New Zealand). *Palaios* **2009**, *24*, 92–103. [[CrossRef](#)]
24. Bracchi, V.A.; Caronni, S.; Meroni, A.N.; Burguett, E.G.; Atzori, F.; Cadoni, N.; Marchese, F.; Basso, D. Morphostructural Characterization of the Heterogeneous Rhodolith Bed at the Marine Protected Area “Capo Carbonara” (Italy) and Hydrodynamics. *Diversity* **2022**, *14*, 51. [[CrossRef](#)]
25. Jardim, V.L.; Gauthier, O.; Toumi, C.; Grall, J. Quantifying maerl (rhodolith) habitat complexity along an environmental gradient at regional scale in the Northeast Atlantic. *Mar. Environ. Res.* **2022**, *181*, 105768. [[CrossRef](#)]
26. Basso, D.; Vrsaljko, D.; Grgasović, T. The coralline flora of a Miocene maerl: The Croatian “Litavac”. *Geol. Croat.* **2008**, *61*, 333–340. [[CrossRef](#)]
27. Bassi, D.; Nebelsick, J.H.; Checconi, A.; Hohenegger, J.; Iryu, Y. Present-day and fossil rhodolith pavements compared: Their potential for analysing shallow-water carbonate deposits. *Sediment. Geol.* **2009**, *214*, 74–84. [[CrossRef](#)]
28. Gagnon, P.; Matheson, K.; Stapleton, M. Variation in rhodolith morphology and biogenic potential of newly discovered rhodolith beds in Newfoundland and Labrador (Canada). *Bot. Mar.* **2012**, *55*, 85–99. [[CrossRef](#)]
29. De Queiroz, E.V.; Araújo, P.V.D.N.; Hammill, E.; Amaral, R.F.D. Morphological characteristics of rhodolith and correlations with associated sediment in a sandstone reef: Northeast Brazil. *Reg. Stud. Mar. Sci.* **2016**, *8*, 133–140. [[CrossRef](#)]
30. Bracchi, V.A.; Angeletti, L.; Marchese, F.; Taviani, M.; Cardone, F.; Hajdas, I.; Grande, V.; Prampolini, M.; Caragnano, A.; Corselli, C.; et al. A resilient deep-water rhodolith bed off the Egadi Archipelago (Mediterranean Sea) and its actual paleontological significance. *Alp. Mediterr. Quat.* **2019**, *32*, 1–20.
31. Basso, D. Deep rhodolith distribution in the Pontian Islands, Italy: A model for the paleoecology of a temperate sea. *Palaeogeogr. Palaeoclim. Palaeoecol.* **1998**, *137*, 173–187. [[CrossRef](#)]
32. Bosence, D.W.J. Description and Classification of Rhodoliths (Rhodoids, Rhodolites). In *Coated Grains*; Peryt, T.M., Ed.; Springer: Berlin/Heidelberg, Germany, 1983; pp. 217–224.
33. Carvalho, V.F.; Assis, J.; Serrão, E.A.; Nunes, J.M.; Anderson, A.B.; Batista, M.B.; Barufi, J.B.; Silva, J.; Pereira, S.M.; Horta, P.A. Environmental drivers of rhodolith beds and epiphytes community along the South Western Atlantic coast. *Mar. Environ. Res.* **2019**, *154*, 104827. [[CrossRef](#)]
34. Adey, W.H.; Macintyre, I.G. Crustose Coralline Algae: A Re-evaluation in the Geological Sciences. *GSA Bull.* **1973**, *84*, 883–904. [[CrossRef](#)]
35. Steller, D.L.; Foster, M.S. Environmental factors influencing distribution and morphology of rhodoliths on Bahía Concepción, B.C.S, México. *J. Exp. Mar. Biol. Ecol.* **1995**, *194*, 201–212. [[CrossRef](#)]
36. Lund, M.; Davies, P.J.; Braga, J.C. Coralline algal nodules off Fraser Island, eastern Australia. *Facies* **2000**, *42*, 25–34. [[CrossRef](#)]
37. Foster, M.S.; Riosmena-Rodriguez, R.; Steller, D.L.; Woelkerling, W.J. Living rhodolith beds in the Gulf of California and their implications. In *Pliocene Carbonates and Related Facies Flanking the Gulf of California, Baja California, Mexico*; Special Paper; Johnson, M.E., Ledesma-Vazquez, J., Eds.; Geological Society of America: Boulder, CO, USA, 1997; pp. 27–139.
38. Minnery, G.A.; Rezak, R.; Bright, T.J. Depth Zonation and Growth Form of Crustose Coralline Algae: Flower Garden Banks, Northwestern Gulf of Mexico. In *Paleoalgeology: Contemporary Research and Applications*; Toomey, D.F., Nitecki, M.H., Eds.; Springer: Berlin/Heidelberg, Germany, 1985; pp. 237–247.
39. Amado-Filho, G.M.; Maneveldt, G.; Manso, R.C.C.; Marins Rosa, B.V.; Pacheco, M.R. Guimarães SMPB 2007 Structure of rhodolith beds from 4 to 55 meters deep along the southern coast of Espírito Santo State, Brazil. *Cienc Mar* **2007**, *33*, 399–410. [[CrossRef](#)]
40. Littler, M.M.; Littler, D.S.; Hanisak, M.D. Deep-water rhodolith distribution, productivity and growth history at sites of formation and subsequent degradation. *J. Mar. Biol. Ecol.* **1991**, *150*, 163–182. [[CrossRef](#)]
41. Basso, D.; Brusoni, F. The molluscan assemblage of a transitional environment: The Mediterranean maerl from off the Elba Island (Tuscan Archipelago, Tyrrhenian Sea). *Boll. Malacol.* **2004**, *40*, 37–45.
42. Staff, G.; Powell, E. The paleoecological significance of diversity: The effect of time averaging and differential preservation on macroinvertebrate species richness in death assemblages. *Palaeogeogr. Palaeoclim. Palaeoecol.* **1988**, *63*, 73–89. [[CrossRef](#)]
43. Kidwell, S.M. Time-averaging in the marine fossil record: Overview of strategies and uncertainties. *GEOBIOS* **1998**, *30*, 977–995. [[CrossRef](#)]
44. Basso, D.; Corselli, C. Molluscan Paleoecology in the Reconstruction of Coastal Changes. In *Black Sea Flood Question: Changes in Coastline, Climate, and Human Settlement*; NATO Science Series IV, Earth and Environmental Science; Yanko-Hombach, V., Gilbert, A.S., Panin, N., Dolukhanov, P.M., Eds.; Kluwer Academic Press: Dordrecht, The Netherlands, 2007; pp. 23–46.
45. Bracchi, V.A.; Nalin, R.; Basso, D. Paleoecology and dynamics of coralline-dominated facies during a Pleistocene transgressive-regressive cycle (Capo Colonna marine terrace, Southern Italy). *Palaeogeogr. Palaeoclimatol. Palaeoecol.* **2014**, *414*, 296–309. [[CrossRef](#)]

46. Bracchi, V.A.; Nalin, R.; Basso, D. Morpho-structural heterogeneity of shallow-water coralligenous in a Pleistocene marine Terrace (Le Castella, Italy). *Palaeogeogr. Palaeoclimatol. Palaeoecol.* **2016**, *454*, 101–112. [[CrossRef](#)]
47. Petersen, C.G.J. On the animal communities of the sea bottom in the Skagerrak, the Christiania Fjord and the Danish waters. *Rep. Dan. Biol. Stn.* **1915**, *23*, 31–38.
48. Möbius, K. *Die Auster und die Austernwirtschaft*. Wiegandt; Hempel and Parey: Berlin, Germany, 1877; pp. 683–751.
49. Basso, D.; Corselli, C. Community versus biocoenosis in multivariate analysis of benthic molluscan thanatocoenosis. *Riv. It. Paleont. Strat.* **2002**, *108*, 153–172.
50. Pérès, J.M.; Picard, J. Nouveau manuel de bionomie benthique de la Mer Méditerranée. *Recl. De Trav. De La Stn. Mar. D'endoume* **1964**, *31*, 1–137.
51. Pérès, J.M. Major Benthic Assemblages. In *Marine Ecology*; Kinne, O., Ed.; John Wiley and Sons: Hoboken, NJ, USA, 1982; Volume 1, Part 1; pp. 373–522.
52. Official Journal of the European Union. *Directive 2008/56/EC. Directive of the European Parliament and of the Council of 17 June 2008 Establishing a Framework for Community Action in the Field of Marine Environmental Policy (Marine Strategy Framework Directive)*; Official Journal of the European Union: Brussels, Belgium, 2008.
53. Sañé, E.; Ingrassia, M.; Chiocci, F.L.; Argenti, L.; Martorelli, E. Characterization of rhodolith beds-related backscatter facies from the western Pontine Archipelago (Mediterranean Sea). *Mar. Environ. Res.* **2021**, *169*, 105339. [[CrossRef](#)] [[PubMed](#)]
54. Graham, D.J.; Midgley, N.G. Graphical representation of particle shape using triangular diagrams: An Excel spreadsheet method. *Earth Surf. Proc. Landf.* **2000**, *25*, 1473–1477. [[CrossRef](#)]
55. Mediterranean Sea Monitoring and Forecasting Centre. Available online: https://resources.marine.copernicus.eu/product-detail/MEDSEA_MULTIYEAR_PHY_006_004/ (accessed on 15 November 2022).
56. Field, J.G.; Clarke, K.R.; Warwick, R.M. A practical strategy for analysing multispecies distribution patterns. *Mar. Ecol. Prog. Ser.* **1982**, *8*, 37–52. [[CrossRef](#)]
57. Clarke, K.R.; Warwick, R.M. *Change in Marine Communities: An Approach to Statistical Analysis and Interpretation*, 2nd ed.; Primer-E Ltd.: Plymouth, UK, 2001.
58. Basso, D. Considerazioni sulla distribuzione di *Acmaea virginea* (O.F. Müller, 1776) (Gastropoda, Acmaeidae) in tanatocenosi tirreniche. *Bolettino Malacol.* **1992**, *28*, 177–186.
59. Dominici, S. Taphonomy and paleoecology of shallow marine macrofossil assemblages in a collisional setting (late Pliocene-early Pleistocene, western Emilia, Italy). *Palaios* **2001**, *16*, 336–353. [[CrossRef](#)]

Disclaimer/Publisher's Note: The statements, opinions and data contained in all publications are solely those of the individual author(s) and contributor(s) and not of MDPI and/or the editor(s). MDPI and/or the editor(s) disclaim responsibility for any injury to people or property resulting from any ideas, methods, instructions or products referred to in the content.